

A Miniaturised Self-Multiplexing Antenna for Eight Distinct Sub-6 GHz 5G-NR Services for IoT Applications

Gunjan Srivastava^{#,*}, Vimal Kumar[§], Amit Sikder[§], and Akhilesh Mohan[§]

[#]Department of Electronics and Communication Engineering, Graphic Era Deemed to be University, Dehradun-248002, India

[§]Department of Electronics and Communication Engineering, IIT Roorkee, Roorkee-247667, India

*E-mail: gunjansrivastava.ece@geu.ac.in

ABSTRACT

In the realm of fifth-generation (5G) technology, the intelligent deployment of FR1 sub-6 GHz frequency bands provide a significant role in Internet of Things (IoT) based services for smart homes, smart hospitals, smart airports, smart supermarkets, etc. These IoT based services operate in different frequency bands of sub-6 GHz spectrum. For the simultaneous transmission and reception of these signals, self-multiplexing (SM) antennas are one of the best possible solutions. The SM antennas are multiport antennas which operates at several distinct frequencies with high port-to-port isolation. In this paper, a compact Self-Multiplexing (SM) antenna for eight distinct IoT based 5G-NR services is presented. The presented SM antenna consists of four Quarter-Mode Substrate-Integrated-Waveguide (QMSIW) cavities, which are inset fed through four pair of microstrip feedlines to obtain eight distinct frequency bands of 5G-NR services. The design of the proposed antenna is quite flexible in terms of providing independent tunability to each of the operating frequency bands by varying one of the design parameters. The proposed SM antenna radiates at 3.5 GHz (n78), 3.7 GHz (n77), 4.9 GHz (n79), 5.2 GHz (n46), 5.9 GHz (n47), 6.0 GHz (n96), 6.2 GHz (n102) and 6.7 GHz (n104). High inter-port isolation guarantees the good SM characteristics.

Keywords: Internet of things (IoT); Multiport; QMSIW; Cavity backed slot antenna

1. INTRODUCTION

The fifth-generation (5G) communication technology offers enormous connectivity to the various devices through the Internet of Things (IoT)¹⁻². In the recent years, IoT brings drastic change in the life of individuals by providing an inter-connection to wide range of services such as smart home^{3,4}, smart city⁵, intelligent transport systems (ITS), etc. Integrating all these services under the same network is one of the major challenges. To meet the diverse requirements of these services, multistandard and multiband antennas for sub-6 GHz based fifth-generation new radio (5G-NR) bands are required Fig. 1(a).

Several single port single/multiband IoT antennas have been designed and analysed in the literature⁶⁻¹⁰. However, these single port IoT antennas can be used either in the transmit mode or receive mode at an instant. For the simultaneous transmission and reception of the signals in smart devices, multiplexer is being used which in turn increases the system size and complexity. One of the best possible solutions is to use the Self-Multiplexing (SM) IoT antennas. The SM IoT antennas are multiport antennas which operates at several distinct frequencies for various multi-standard IoT services with high port-to-port isolation. Several studies have been performed in the area of SM antennas¹¹⁻²³. Due to inherent advantages of Substrate Integrated Waveguide (SIW) such as low loss, low cost, good port-to-port isolation, ease of

integration with the planar circuits, several self-diplexing¹¹⁻¹³, self-triplexing¹⁴⁻¹⁷, self-quadruplexing¹⁸⁻²⁰, self-pentaplexing²¹ and self-hexaplexing²²⁻²³ based SIW antennas¹⁸⁻²⁰ and are reported in the literature. Thus, for the multi-standard services, designing a compact SM IoT antenna which can operate in a greater number of distinct frequency bands is a great challenge. This motivates the authors to design a multiport self-multiplexing IoT antenna which covers eight distinct frequency bands in FR1 sub-6 GHz spectrum with good port-to-port isolation. These distinct frequencies for 5G-NR applications are provided in Table 1.

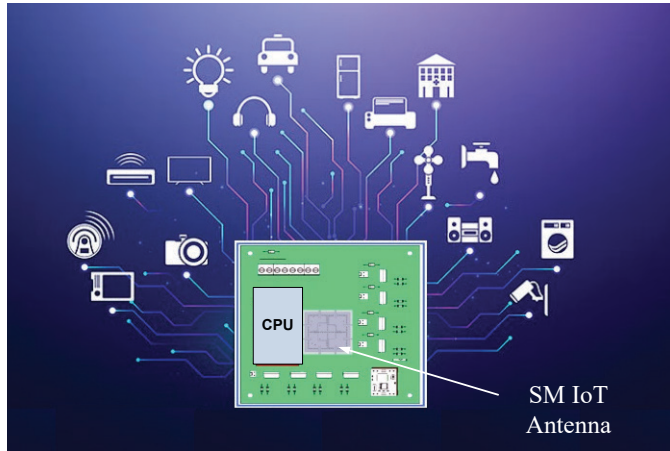
Table 1. 5G-NR bands

NR-Bands	Frequency (MHz)	Applications
n48, n78	3500	Broadcast radio services
n77	3700	Cellular 5G bands
n79	4900	Cellular 5G bands
n46	5200	WLAN /WiFi
n47	5900	V2X communication
n96	6000	U-NII-5-8
n102	6200	U-NII-5
n104	6700	U-NII-6-8

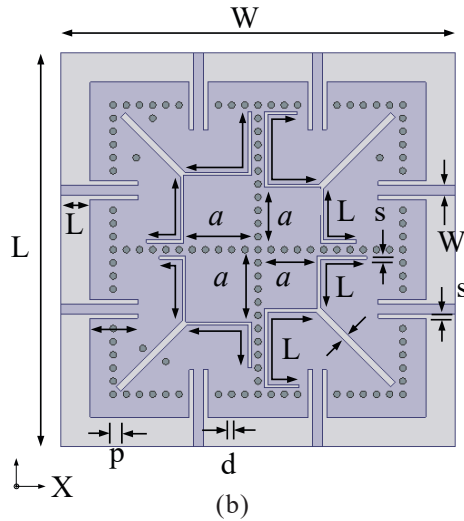
U-NII: Unlicensed Bands mainly used by Wi-Fi 6E devices.

In this work, a compact shielded QMSIW (S-QMSIW) Self-Multiplexing (SM) IoT antenna for eight distinct 5G-NR services such as smart home, smart city, Intelligent Transport Systems (ITS), etc. is presented. By appropriately designing the self-multiplexing IoT antenna along with its feeding

structure eight distinct frequencies of 5G-NR services. are obtained. The novel features of the proposed SM IoT antenna are as follows: (i) To the best of authors' knowledge, it is the first instance when the SM IoT antenna for eight distinct 5G-NR services is proposed. (ii) The operating frequencies of the SM IoT antenna can be tuned independently to other 5G-NR services from 3.5 GHz (n78) to 7.125 GHz (n96, n104) by varying only one design parameter. (iii) The design SM IoT antenna offers high inter-port isolation (>30 dB) along with the compact volume ($0.005 \lambda_g^3$), where λ_g is the lowest operating frequency.



(a)



(b)

Figure 1 (a) Application scenario of proposed self-multiplexing IoT antenna; and (b) Proposed octa-band SM antenna for 5G-NR services.

2. ANTENNA CONFIGURATION

Figure 1(b) shows the geometrical configuration of proposed SM IoT antenna for 5G-NR services. The SM antenna is designed on RT/Duriod substrate with $h=0.508$ mm, $\epsilon_r=2.2$, and $\tan\delta=0.0008$. It comprises of four QMSIW cavity resonators²⁴⁻²⁵. Each of the QMSIW cavity shares two side walls with the adjacent cavities. The diameter d and separation p of vias are selected such that they ensure minimal leakage of energy from the side walls²⁶. These QMSIW resonators are fed through four orthogonal pairs of microstrip feedlines. The feeding ports are designated as P_1, P_2, \dots, P_8 . The diagonal

capacitive slots are introduced in each of QMSIW cavities to provide lower mutual coupling between the ports within the cavity. Moreover, for octa-band operation, two short slots of different lengths are introduced in each of QMSIW cavity.

Table 2. Unloaded Q-factors of SIW resonators

	FMSIW	QMSIW	S-QMSIW
Resonant Freq.	3.29 GHz	3.28 GHz	3.32 GHz
Qu	340.2	264.4	282.3

3. WORKING PRINCIPLE

In this section, the working mechanism of the proposed self-multiplexing IoT antenna for sub-6 GHz 5G NR services is presented.

3.1 Shielded QMSIW Resonator

At the first instance, a full-mode SIW (FMSIW) cavity resonator which operates in TE_{110} mode is being developed Fig. 2(a)]. The operating frequency for TE_{110} mode of the FMSIW cavity resonator is evaluated using the following expression²³:

$$f_{TE_{110}} = \frac{1}{2\pi\sqrt{\mu\epsilon}} \sqrt{\left(\frac{\pi}{L_{eff}}\right)^2 + \left(\frac{\pi}{W_{eff}}\right)^2} \quad (1)$$

where, L_{eff} and W_{eff} are the effective dimensions of the FMSIW cavity that can calculated using the following expressions²³

$$L_{eff} = L - 1.08 \frac{d^2}{s} + 0.1 \frac{d^2}{L} \quad (2)$$

$$W_{eff} = W - 1.08 \frac{d^2}{s} + 0.1 \frac{d^2}{W} \quad (3)$$

where, L and W are length and width of the FMSIW cavity, d is the diameter of the vias and s is the pitch of the vias. In this work, $s=2d$ is chosen for the confinement of the electromagnetic fields within the FMSIW cavity.

To design and develop miniaturized components, the FMSIW cavity resonator can be divided through two magnetic walls AA' and BB' to obtain a compact quarter mode SIW (QMSIW) cavity resonator as shown in Fig. 2(a). With respect to FMSIW cavity resonator, the QMSIW cavity possess radiation losses due to the presence of two open-ended edges (AO and OB'). Further, to minimize this radiation losses, a shielded QMSIW (S-QMSIW) cavity resonator is being developed. In S-QMSIW resonator, the two open-ended edges of QMSIW resonator are replaced with the rows of metallic vias and the required magnetic walls are recreated with the help of the open slots.

The S-QMSIW resonator not only facilitates the size miniaturization but also supports the dominant TE_{110} mode. The unloaded quality factors (Q_u) of FMSIW, QMSIW and S-QMSIW cavity resonators along with their operating frequencies for the dominant TE_{110} mode are depicted in Table 2. These unloaded Q-factors are evaluated with the help of eigenmode solver of Ansys HFSS 2020 R2. It can be concluded from this study that S-QMSIW cavity possess better unloaded Q-factor than the QMSIW cavity resonator, while the resonant frequencies remain almost unaltered.

3.2 Basic Element of SM IoT Antenna

The S-QMSIW resonator is explored for the design of the

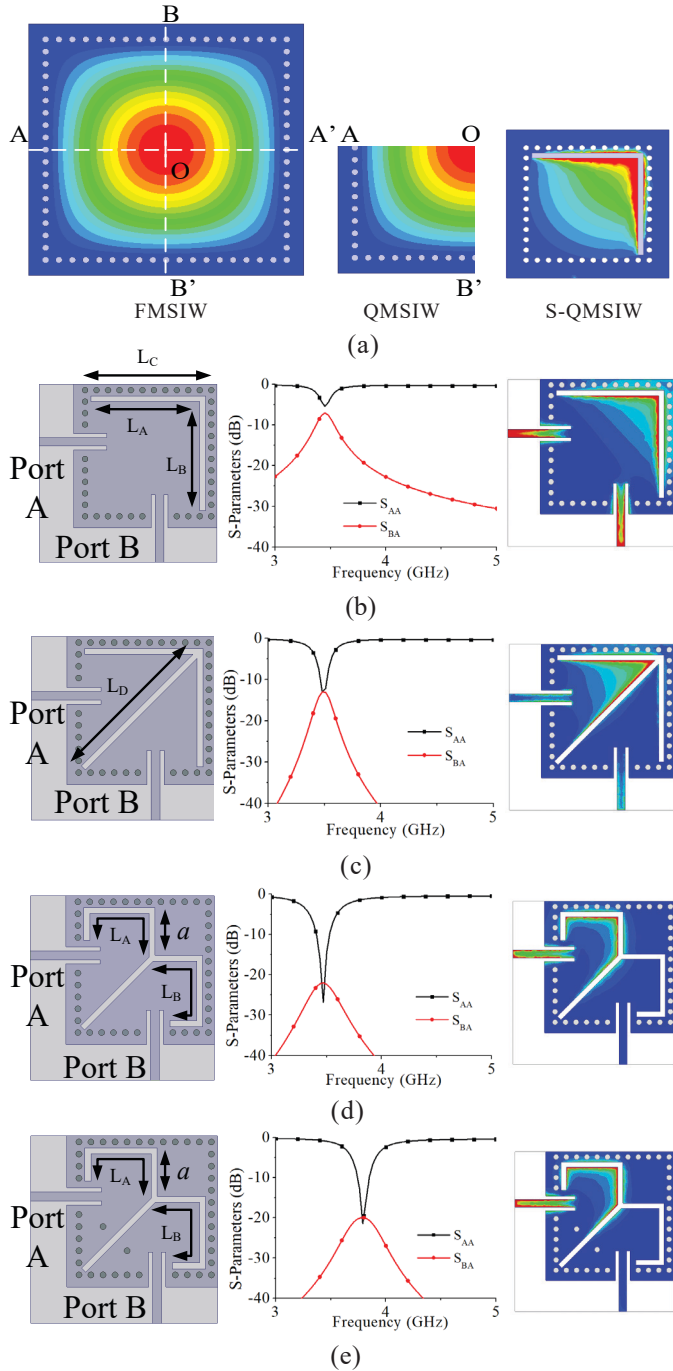


Figure 2. Developmental stages; (a) S-QMSIW cavity resonator; (b) Stage-I; (c) Stage-II; (d) Stage-III; and (e) Stage-IV.

basic element (BE) of the proposed SM antenna. Figure 2(b)-(e) shows the different stages for the design of basic element of SM antenna. In Stage I, the S-QMSIW resonator ($L_C = 22$ mm, $L_A = L_B = 19$ mm, $w_{\text{slot}} = 1$ mm) is fed by a pair of orthogonal microstrip feedlines through Port A and Port B Fig. 2(b)]. The S-QMSIW resonator in Stage I resonates at 3.45 GHz, with substantially high mutual coupling ($|S_{BA}| = -5$ dB) between the two ports Fig. 2(b). To reduce this mutual coupling and improve the impedance matching, a diagonal slot (length $L_D = 26.67$ mm) is created (Stage II). In Stage II, the antenna radiates at 3.48 GHz with mutual coupling ($|S_{BA}| = -12$ dB). However, this mutual coupling is not enough for the antenna to

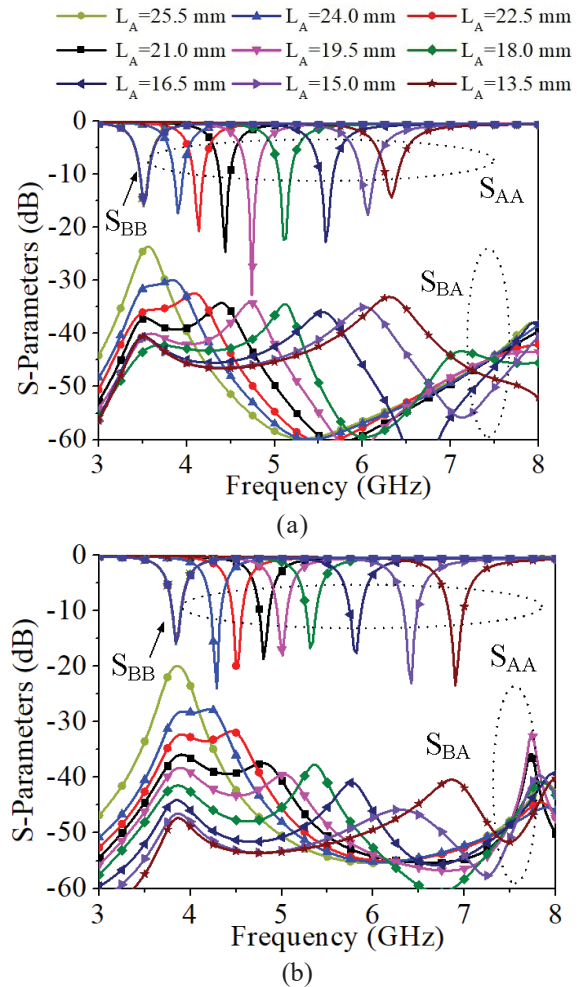


Figure 3. Parametric analysis of (a) design parameter L_A in Stage-III (without via); and (b) design parameter L_A in Stage-IV (with via).

operate in self-multiplexing (SM) mode. Further, to lower the mutual coupling, short slots and a square patch of dimension $a \times a$ are incorporated in Stage III ($L_A = L_B = 25.5$ mm, $a = 8$ mm) as shown in Fig. 2(d). The antenna in Stage III radiates at 3.5 GHz with $|S_{BA}| = -20$ dB. This antenna is our basic element for the lower 5G-NR bands.

To get better insight of the dependency of the resonant frequencies on the design parameter L_A in Stage III, a parametric study is performed and their results are analysed. Figure 3(a) shows the S-parameters of the Stage III for the different values of L_A (for $L_B = 25.5$ mm). As the slot length L_A increases, the capacitance of the open-ended part of the resonator increases, which increases the total equivalent capacitance of the resonator. This additional capacitance increases the equivalent path for the signal that in turns lowers the resonant frequency. When L_A is varied from 25.5 mm to 13.5 mm, the operating frequency of the respective port (Port A) changes from 3.50 GHz to 6.3 GHz, while the resonant frequency of other port (Port B) remains unaltered. This ensures the advantage of independent tunability of the operating frequency of the basic antenna element by varying L_A . The isolation between the ports for $L_A = L_B = 25.5$ mm is nearly 12 dB.

For the SM operation, the values of L_A and L_B should be different, which will provide different capacitances that in

Table 3. Frequency tuning range

Parameter range (mm)	Frequency range (GHz)
$18.0 \leq L_1 \leq 23.0$	3.54 – 4.40
$10.3 \leq L_2 \leq 16.3$	4.34 – 6.00
$8.7 \leq L_3 \leq 16.7$	4.70 – 6.56
$12.8 \leq L_4 \leq 22.8$	3.66 – 5.42
$12.8 \leq L_5 \leq 18.8$	5.98 – 6.40
$12.8 \leq L_6 \leq 18.8$	5.38 – 6.88
$11.8 \leq L_7 \leq 15.8$	5.80 – 7.05
$14.8 \leq L_8 \leq 17.8$	5.60 – 6.55

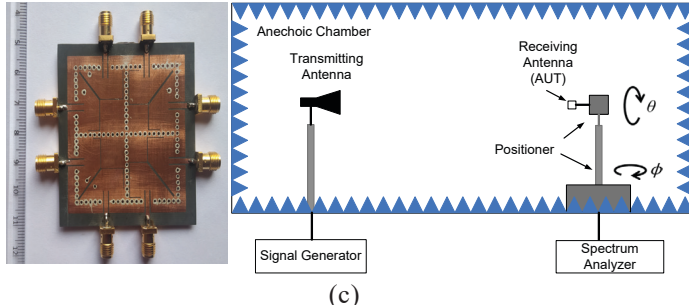
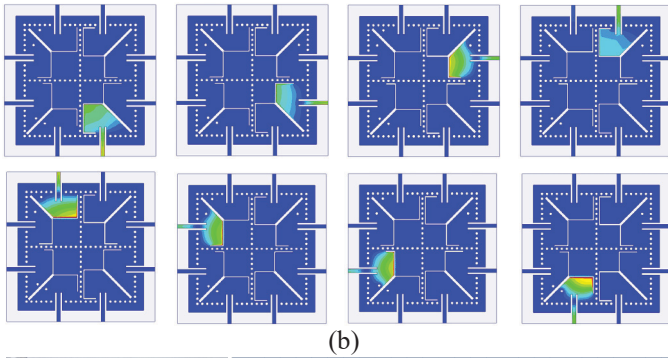
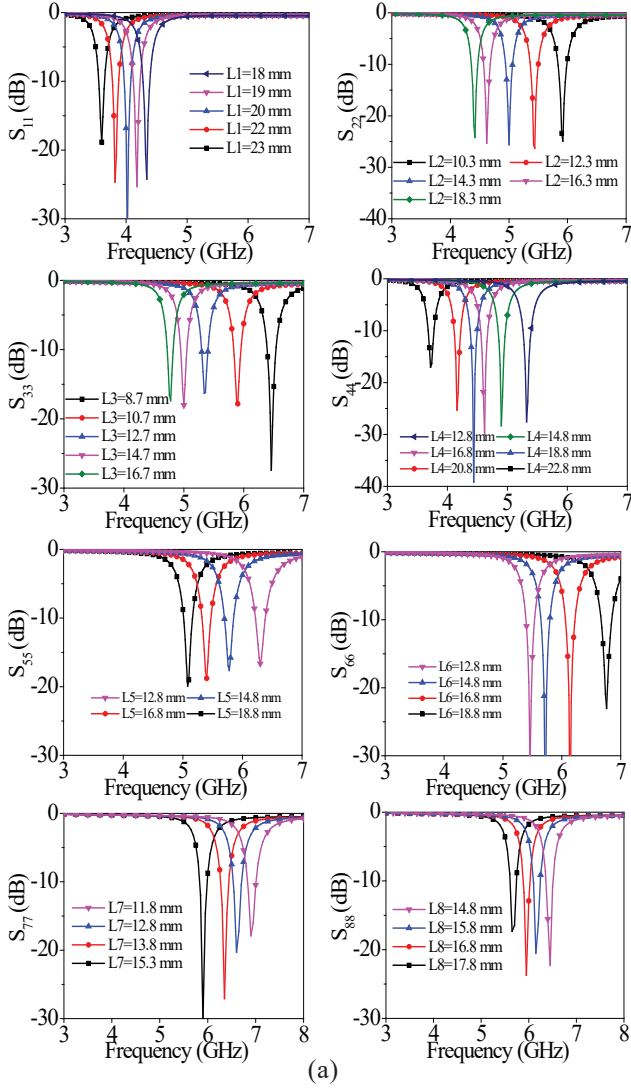


Figure 4. (a) Frequency tuning range for each port; (b) E-field distribution when the respective ports are ON. The other remaining ports are terminated with matched loads; (c) Photograph of the fabricated prototype and experimental Setup for the measurement of radiation pattern.

turn results in different SM frequencies. As the value of L_A changes, keeping LB constant, provides the unequal lengths that in turn improves the inter-port isolation. The frequencies for lower 5G-NR bands can be obtained with the variation of L_A . However, the higher 5G-NR frequencies cannot be obtained by the variation of parameter L_A .

Further, to facilitates the radiations at higher 5G-NR frequencies, two vias are introduced near the diagonal slot [Stage IV, Fig. 2(e)]. These vias effectively increase the inductance which shift the operating frequency to the higher values. Figure 3(b) shows the parametric study of the design parameter L_A with the presence of two vias in Stage IV, keeping other design parameters constant. It can be observed from the figure that as the value of L_A changes from 25.5 mm to 13.5 mm, the radiating frequency of the respective port (Port A) shift to higher values (nearly up to 7 GHz), while the radiating frequency of other port (Port B) remains unaltered.

The resonant frequency in Stage IV can be independently tuned by 3.8 GHz to 7.0 GHz by varying the design parameter L_A from 25.5 mm to 13.5 mm along with high inter-port isolation. It is worth mentioning here that the unequal lengths of L_A and L_B , not only provides the different operating frequencies for SM operation, but also enhances the inter-port isolation as well.

3.3 Proposed SM IoT Antenna

The geometrical configuration of our proposed SM IoT antenna for 5G-NR services is shown Fig. 1(a). It consists of basic elements (BE) developed in the above sub-section. The basic element depends upon the required frequencies of 5G-NR bands. The self-multiplexing (SM) operation at the lower n48, n78 bands (3.5 GHz) and n79 band (4.9 GHz) is achieved through the usage of Stage-III as a basic element in proposed SM antenna. The SM antenna radiates at 3.5 GHz when port P_1 is ON and 4.9 GHz, when port P_2 is ON, the other unused ports are terminated with 50 Ω matched loads. The low mutual coupling $|S_{21}| = -30$ dB is obtained due to the asymmetrical length of the slots. For SM behavior at n77 (3.7 GHz) and n49 (5.9 GHz) bands, the Stage III is used as basic element. When the SM antenna is fed through port P_4 , it radiates at 3.7 GHz. To obtain the radiations at 5.9 GHz (when port P_3 is ON), a via is introduced inside the cavity that in turn shifts the resonant frequency to higher value Fig. 3(b)]. With the introduction of this via, the SM antenna radiates at 5.9 GHz, when fed through port P_3 , along with the isolation better than 30 dB between the ports P_3 and P_4 .

Table 4. Comparison with other reported SM antennas

Ref	Freq (GHz)	Isolation (dB)	Gain (dBi)	Size (λ_g^3)	Operation
13	8.19,8.8,9.7,11	>22	5.5,6.9,7.47,7.45	0.792	Quad-Band
14	2.45,3.5,4.9,5.4	>29	3.85,5.33,5.95,5.97	0.23	Quad-Band
15	4.35,5.35,5.9,6.75	>27	4.04,4.48,4.55,6.12	0.16	Quad-Band
16	2.29,2.98,3.65,4.37,5.08	>29	3.59,4.55,3.91,5.7,4.92	0.173	Penta-band
17	5.33,5.76,6.31,6.86,7.34,7.8	>24	4.5,4.94,4.9,5.12,6.12,6.6	0.39	Hexa-band
18	2.29,2.96,4.30,5.0,5.61,6.18	>27	3.73,4.35,5.57,5.46,4.73	0.173	Hexa-band
Prop.	3.46, 3.69, 4.84, 5.2, 5.88, 5.95, 6.16, 6.65	>30	4.96, 5.17, 5.97, 5.87, 6.06, 5.86, 5.93, 6.64	0.005	Octa-band

λ_g is the guided wavelength at the lowest operating frequency

Further, for the SM behavior at n46 (5.2 GHz) and n102 (6.2 GHz) bands, Stage IV is chosen as the basic element. When the port P_5 is ON, the SM antenna radiates at 5.2 GHz when the port P_6 is ON, it radiates at 6.2 GHz. The low mutual coupling $|S_{65}| = -30$ dB is also obtained between the ports P_5 and P_6 . In the similar fashion, the SM performance at n96 (6.0 GHz, when port P_7 is ON) and n104 (6.7 GHz, when port P_8 is ON) bands are obtained. The isolation between the ports P_7 and P_8 is also better than 30 dB. It is important to note that the difference in radiating frequencies within a basic element is approximately 1 GHz that will provide different slot lengths (L_A, L_B) which ensures high inter-port isolation within the cavity.

3.4 Frequency Tuning Range

The frequency tunability of each port of the proposed self-multiplexing antenna can be obtained by varying the respective lengths of the slots (L_i 's of the i^{th} port). Figure 4(a) demonstrates the agility of the frequencies with respect to design parameters L_i ($i=1,2,..8$). For example, the variation of S_{11} with respect to L_1 can be observed in Fig. 4(a), while all other design parameters remain unaltered. As the value of L_1 increases from 18 mm to 23 mm, the resonant frequency of port P_1 varies from 4.40 GHz to 3.54 GHz, that finds its applications in various new radio (NR) bands of the 5G spectrum. Table 3 shows the frequency tuning range of each port for different values of L_i 's. Thus, this frequency tuning range permits the designed self-multiplexing antenna to operate at the designated eight frequencies within the above tabulated tuning ranges, that facilitates its application in several IoT devices that operates in 5G NR bands.

3.5 Electric Field Distribution

Figure 4(b) shows electric field distribution of the proposed SM antenna at the eight distinct operating frequencies, when the excitation is applied at their respective ports, while the other unused ports are terminated with the matched loads. It is apparent from the electric field distributions that each QMSIW cavity resonator operates in fundamental TE_{110} mode, without transmitting any fields to the neighbouring QMSIW resonators resulting in high isolation among all the ports.

3.6 Design Guidelines

Based on the aforementioned studies, the following guidelines are provided for the design of the proposed self-multiplexing antenna for IoT applications:

- Realize a square SIW cavity with a dimension $L \times W$ that supports the TE_{110} mode.
- Bisect the square SIW cavity twice across the symmetrical planes to obtain a QMSIW cavity resonator.
- Apply the vias and narrow slots across the open-ended edges of the QMSIW cavity resonator to obtain the shielded QMSIW (S-QMSIW) resonator.
- Feed the S-QMSIW resonator orthogonally through a pair of microstrip feedlines. Place a diagonal slot in S-QMSIW resonator to obtain good isolation between the two feeding ports.
- Add a square patch near the open-edges of the S-QMSIW resonator for impedance match at the operating frequencies.
- Engrave additional rectangular slots near the open-ended edges to shift (lowering) the frequencies of the resonators to the desired bands.
- Add vias to the resonators to increasing the frequencies of the resonators for higher frequencies of the self-multiplexing antenna.
- Four S-QMSIW resonators are placed side by side a form the proposed self-multiplexing antenna for IoT applications.
- Due to usage of S-QMSIW resonators, high inter-port isolations are obtained.

The final design parameters are as follows (in mm): $L = 60$, $W = 60$, $L_{f1} = 4.5$, $L_{f2} = 7.35$, $W_f = 1.48$, $s = 0.76$, $s_1 = 1$, $s_2 = 0.5$, $d = 1$, $p = 2$, $L_1 = 25.5$, $L_2 = 15.5$, $L_3 = 13.9$, $L_4 = 25$, $L_5 = 20$, $L_6 = 16$, $L_7 = 14$, $L_8 = 17$, $a_1 = 8.0$, $a_2 = 8.5$, $a_3 = 10.3$, $a_4 = 9$.

4. RESULTS AND DISCUSSION

A prototype of the designed SM antenna has been fabricated using standard PCB process and SMA connectors are soldered at all the ports for measurement purposes. The dielectric substrate RT/Duroid 5880 having dielectric constant 2.2, loss tangent 0.0008 and thickness 0.508 mm is used for the fabrication of the SM antenna. The photograph of the fabricated SM antenna is shown in Fig. 4(c). The SM antenna has overall dimensions of 60 mm×60 mm×0.508 mm. Agilent 5071C vector network analyzer is used to measure the S-parameters and anechoic chamber is used to measure the radiation characteristics of the SM antenna. Figure 5(a) shows the simulated and measured reflection coefficients of the designed SM antenna. The fabricated antenna radiates at 3.46 GHz, 4.84 GHz, 5.88 GHz, 3.69 GHz, 5.15 GHz, 6.17 GHz, 5.96 GHz, 6.65 GHz while their simulated operating

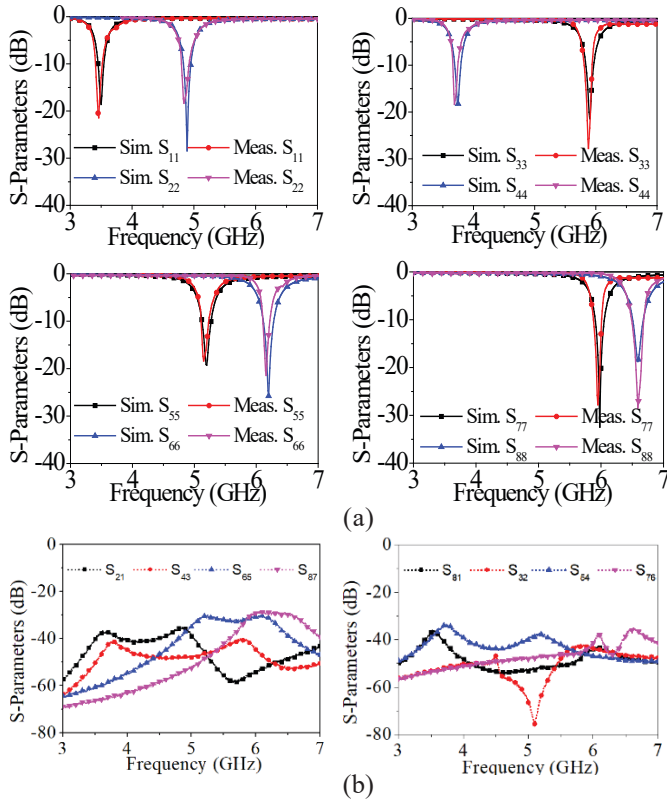


Figure 5. (a) Simulated and measured reflection coefficients; and (b) Measured transmission coefficients.

frequencies are 3.5 GHz, 4.90 GHz, 5.90 GHz, 3.70 GHz, 5.20 GHz, 6.2 GHz, 6.0 GHz and 6.70 GHz. The isolation is better than 30 dB among all the ports. For brevity, the measured transmission coefficients of adjacent ports are provided in Figure 5(b) and they are below -30 dB.

The experimental setup for the measurement of far-field radiation pattern is shown in Fig. 4(c). The simulated and measured far-field normalized radiation patterns of the designed SM antenna in both the principal planes, i.e. E-plane and H-plane are plotted in Fig. 6 for each port excitation. During the measurement of one each port, the other unused ports are terminated with matched loads. The measured peak gains of SM are 4.96 dBi, 5.97 dBi, 6.06 dBi, 5.17 dBi, 5.87 dBi, 5.93 dBi, 5.86 dBi, 6.64 dBi at the corresponding operating frequencies of 3.46 GHz, 4.84 GHz, 5.88 GHz, 3.69 GHz, 5.15 GHz, 6.17 GHz, 5.96 GHz, 6.65 GHz. The radiation efficiencies are above 83 % for all the operating frequencies.

To demonstrate the benefits of the proposed SM IoT antenna, a comparison has been made with the other reported SM antennas in the literature and is presented in Table 4. The unique characteristics such as compact dimensions, good peak gains, octa-band operation and high port-to port isolation with independent frequency tunability of the designed SM antenna makes it a good candidate for IoT based 5G-NR services. Moreover, to the best of authors' knowledge, this is the first instance where the compact octa-band SM antenna for IoT based 5G-NR services has been reported.

5. CONCLUSIONS

In this paper, a systematic approach to design a compact eight port self-multiplexing IoT antenna for

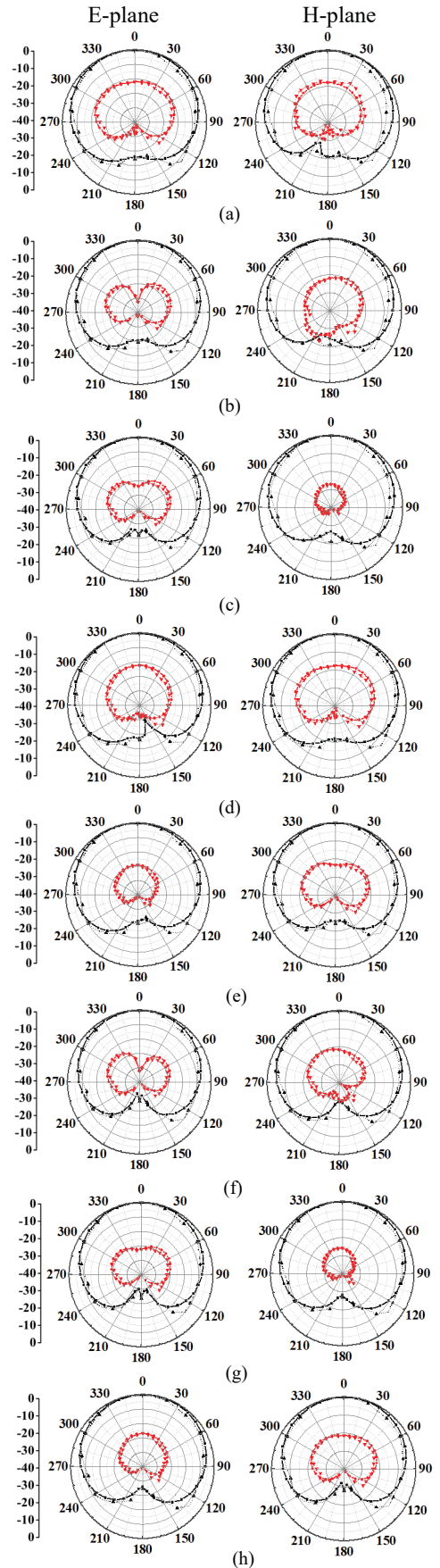


Figure 6. Simulated and measured radiation patterns at their respective operating frequencies; (a) P_1 ON; (b) P_2 ON; (c) P_3 ON; (d) P_4 ON; (e) P_5 ON; (f) P_6 ON; (g) P_7 ON; and (h) P_8 ON.

5G-NR services is presented for the first instance. The SM IoT antenna radiates at eight distinct frequency bands from 3.5 GHz to 6.7 GHz (3.46, 3.69, 4.84, 5.2, 5.88, 5.95, 6.16, 6.65 GHz) for various smart devices. The designed IoT antenna can be independently tuned to other 5G-NR services from 3.5 GHz (n78) to 7.125 GHz (n96, n104) by varying one design parameter. This SM IoT antenna also offers high inter-port isolation better than 30 dB. The operating principle of designed SM IoT antenna is presented in detail. With an advantage of independent frequency tunability and high inter-port isolation within the compact dimensions make it a potential candidate for various IoT devices operating in sub-6 GHz 5G spectrum.

REFERENCES

- Chettri, L. & Bera, R. A comprehensive survey on Internet of Things (IoT) toward 5G wireless systems. *IEEE Internet Things J.*, 2020, **7**(1), 16–32.
- Jia, R.; Chen, X.; Qi, Q. & Lin, H. Massive beam-division multiple access for B5G cellular internet of things. *IEEE Internet Things J.*, 2020, **7**(3), 2386–2396.
- Li, W.; Logenthiran, T.; Phan, V.T. & Woo, W.L. A novel smart energy theft system (SETS) for IoT-based smart home. *IEEE Internet Things J.*, 2019, **6**(3), 5531–5539.
- Huang, Z.; Zhang, L.; Meng, X. & Choo, K.-K. R. Key-free authentication protocol against subverted indoor smart devices for smart home. *IEEE Internet Things J.*, 2020, **7**(2), 1039–1047.
- Zanella, A.; Bui, N.; Castellani, A.; Vangelista, L. & Zorzi, M. Internet of Things for smart cities. *IEEE Internet Things J.*, 2014, **1**(2), 22–32.
- Mehdipour, A.; Sebak, A.; Trueman, C.W. & Denidni, T.A. Compact multiband planar antenna for 2.4/3.5/5.2/5.8-GHz wireless applications. *IEEE Antennas Wireless Propag. Lett.*, 2012, **11**, 144–147.
- Islam, M.S.; Islam, M.T.; Ullah, M.A.; Beng, G.K.; Amin, N. & Misran, N. A modified meander line microstrip patch antenna with enhanced bandwidth for 2.4 GHz ISM-band Internet of Things (IoT) applications. *IEEE Access*, 2019, **7**, 127850–127861.
- Bichara, R.M.; Asadallah, F.A.; Costantine, J. & Awad, M.A. folded miniaturized antenna for IoT devices”, *Proc. IEEE Conf. Antenna Meas. Appl.*, 2018.
- Su, Z.; Klionovski, K.; Bilal, R.M. & Shamim, A. 3D printed antenna-on-package with near-isotropic radiation pattern for IoT (WiFi based) applications”, *Proc. IEEE Int. Symp. Antennas Propag. USNC/URSI Nat. Radio Sci. Meeting*, 2018.
- Bekasiewicz, A. & Koziel, S. Compact UWB monopole antenna for Internet of Things applications. *Electron. Lett.*, 2016, **52**(7), 492–494.
- Romputtal, A. & Phongcharoenpanich, C. IoT-linked integrated NFC and dual band UHF/2.45 GHz RFID reader antenna scheme. *IEEE Access*, 2019, **7**, 177832–177843.
- Mukherjee, S. & Biswas, A. Design of Self-Diplexing Substrate Integrated Waveguide Cavity-Backed Slot Antenna. *IEEE Antennas Wireless Propag. Lett.*, 2016, **15**, 1775–1778.
- Nandi, S. & Mohan, A. An SIW Cavity-Backed Self-Diplexing Antenna. *IEEE Antennas Wireless Propag. Lett.*, 2017, **16**, 2708–2711.
- Pradhan, N.C.; Subramanian, K.S.; Barik, R.K.; Dalal, P. & Cheng, Q.S. Design of compact shielded QMSIW based self-diplexing antenna for high-isolation. *Proc. IEEE Wireless Antenna Microw. Symp.*, 2022, pp. 1–4.
- Priya, S. & Dwari, S. A compact self-triplexing antenna using HMSIW cavity. *IEEE Antennas Wireless Propag. Lett.*, 2020, **19**(5), 861–865.
- Iqbal, A.; Selmi, M.A.; Abdulrazak, L.F.; Saraereh, O.A.; Mallat, N.K. & Smida A. A compact substrate integrated waveguide cavity-backed self-triplexing antenna. *IEEE Trans. Circuits Syst. II, Exp. Briefs*, 2020, **67**(11), 2362–2366.
- Mukherjee, S.; Ghosh, S. & Biswas, A. Design of compact SIW cavity backed self-triplexing planar slot antenna for triple band application. In 2021 15th European Conference on Antennas and Propagation (EuCAP), Dusseldorf, Germany, 2021.
- Kumar, A.; Kumar, M. & Singh, A.K. On the behavior of self-triplexing SIW cavity backed antenna with non-linear replicated hybrid slot for C and X-Band applications. *IEEE Access*, 2022, **10**, 22952–22959.
- Priya, S.; Dwari, S.; Kumar, K. & Mandal, M.K. Compact self-quadruplexing SIW cavity-backed slot antenna. *IEEE Trans. on Antenn. and Prop.*, 2019, **67**(10), 6656–6660.
- Iqbal, A.; Tiang, J. J.; Wong, S.K.; Wong, S.W. & Mallat, N.K. SIW cavity-backed self-quadruplexing antenna for compact RF front ends. *IEEE Antennas Wireless Propag. Lett.*, 2021, **20**(4), 562–566.
- Iqbal, A.; Al-Hasan, M.; Mabrouk, I.B. & Denidni, T.A., Highly miniaturised eighth-mode substrate-integrated waveguide self-quadruplexing antenna. *IEEE Antennas Wireless Propag. Lett.*, 2023, **22**(9), 2275–2279.
- Barik, R.K. & Koziel, S. Design of compact self-quintuplexing antenna with high-isolation for penta-band applications. *IEEE Access*, 2023, **11**, 30899–30907.
- Dash, S.K.K.; Cheng, Q.S.; Barik, R.K.; Jiang, F.; Pradhan, N.C. & Subramanian, K.S. A compact siw cavity-backed self-multiplexing antenna for hexa-band operation. *IEEE Trans. on Antenn. and Prop.*, 2022, **70**(3), 2283–2288.
- Barik, R.K. & Koziel, S. A compact self-hexaplexing antenna implemented on substrate-integrated rectangular cavity for hexa-band applications. *IEEE Trans. Circuits Syst. II, Exp. Briefs*, 2023, **70**(2), 506–510.
- Wang, X.; Zhu, X. -W.; Tian, L.; Liu, P.; Hong, W. & Zhu, A., Design and experiment of filtering power divider based on shielded HMSIW/QMSIW technology for 5G wireless applications. *IEEE Access*, 2019, **7**, 72411–72419.
- Zheng, Y.; Zhu, Y.; Wang, Z. & Dong, Y. Compact, Wide stopband, shielded hybrid filter based on quarter-mode substrate integrated waveguide and microstrip line resonators. *IEEE Microwave and Wireless Components Lett.*, 2021, **31**(3), 245–248.
- Bozzi, M.; Georgiadis, A. & Wu, K. Review of substrate-

integrated waveguide circuits and antennas. *IET Microw., Antennas Propag.*, 2011, **5**(8), 909–920.

CONTRIBUTORS

Dr Gunjan Srivastava obtained her PhD degree from the IIT, Dhanbad, India in Microwave Engineering and working as Associate Professor in the Department of Electronics and Communication Engineering at Graphic Era (Deemed to be) University, Dehradun. Her main research interests are design of ultra-wideband, reconfigurable, differential, SIW, MIMO and self-multiplexing antennas.

In the current study she has contributed in terms of conceptualisation, simulation, fabrication, measurements, and manuscript writing.

Mr Vimal Kumar obtained his MTech degree from the Department of Avionics, Indian Institute of Space Science and Technology Thiruvananthapuram, India. Currently, he is pursuing a PhD from the Department of Electronics and Communication Engineering, IIT Roorkee, India. His research interests are space-fed high-

gain antennas, MIMO antennas, and passive microwave circuits. In the current study he contributed in terms of fabrication and measurements.

Mr Amit Sikder obtained his MTech. degree from the Department of Electronics and Communication Engineering, IIT Roorkee, India. His research interests are high -gain antennas, MIMO antennas, and passive microwave circuits.

In the current study he has contributed in terms of fabrication and measurements.

Dr Akhilesh Mohan obtained his PhD degree in Microwave Engineering from IIT Kanpur and working as a Faculty Member in Department of Electronics and Communication Engineering at IIT Roorkee. His research interests include: Design of microwave filters, antennas, and absorbers for wireless communication systems.

In the current study he contributed as conceptualisation and manuscript-editing.